Journal of Organometallic Chemistry 693 (2008) 3303–3311

Contents lists available at ScienceDirect

Journal of Organometallic Chemistry

journal homepage: www.elsevier.com/locate/jorganchem

# Synthesis, fluxional behavior, and *endo*, *exo*-stereoisomers of allyl molybdenum complexes with *O*-ethyldithiocarbonate, $EtOCS_2^-$, containing ligand: Crystal structures of $[Mo(CH_3CN)(\eta^3\text{-}C_3H_5)(CO)_2(S_2COEt)]$, *exo*-$[Mo(dppm)(\eta^3\text{-}C_3H_5)(CO)(S_2COEt)]$, and *endo*-, *exo*-$[Mo(dppa)(\eta^3\text{-}C_3H_5)(CO)(S_2COEt)]$

Kuang-Hway Yih [a,*], Gene-Hsiang Lee [b]

[a] *Department of Applied Cosmetology, Hungkuang University, No. 34, Chung Chie Road, Shalu, Taichung Hsien, Taiwan 433, ROC*
[b] *Instrumentation Center, College of Science, National Taiwan University, Taiwan, ROC*

ARTICLE INFO

*Article history:*
Received 14 May 2008
Received in revised form 21 July 2008
Accepted 22 July 2008
Available online 29 July 2008

*Keywords:*
*endo*
*exo*-Stereoisomers
Allyl
Molybdenum
O-Ethyldithiocarbonate
Crystal structures

ABSTRACT

The very air-sensitive $\eta^3$-allyldicarbonylethoxydithiocarbonate molybdenum(II) compound $[Mo(\eta^3\text{-}C_3H_5)(CO)_2(S_2COEt)(CH_3CN)]$ (**1**) are accessible by the reaction of $[Mo(\eta^3\text{-}C_3H_5)(CO)_2(Br)(CH_3CN)_2]$ with $KS_2COEt$ in methanol at ambient temperature. The rotational behavior of **1** in solution state was detected by variable-temperature $^1H$ NMR spectroscopy. The mechanism can be described as a trigonal twist, in which the rotation of the triangular face formed by the nitrogen ligand and the two sulfur atoms relative to the face formed by the allyl and the two carbonyl groups. The reactions of **1** with piperidine, 1-piperidinecarbodithioate, and bipyridine ligands give the replacement of the acetonitrile complex $[Mo(\eta^3\text{-}C_3H_5)(CO)_2(S_2COEt)(C_5H_{10}NH)]$ (**2**), 16-electron complex $[Mo(\eta^3\text{-}C_3H_5)(CO)_2(S_2CNC_5H_{10})]$ (**3**), and $\eta^1$-*O*-ethyldithiocarbonate complex $[Mo(\eta^3\text{-}C_3H_5)(CO)_2(S_2COEt)(bipy)]$ (**4**). Treatment of **1** with various diphos ligands form a mixtures of *endo*- and *exo*-complexes $[Mo(\eta^3\text{-}C_3H_5)(S_2COEt)(CO)(diphos)]$ (diphos: dppm = {bis(diphenylphosphino)methane} (*endo*-, *exo*-**5**); dppe = {1,2-bis(diphenylphosphino)ethane} (*endo*-, *exo*-**6**); dppa = {bis(diphenylphosphino)amine} (*endo*-, *exo*-**8**)) with ratios of 1:5, 1:2, and 4:5 according to the integration of $^{31}P\{^1H\}$ NMR spectra, respectively. The orientations of *endo* and *exo* are defined for the open face of the allyl group and carbonyl group in the same direction in the former and opposite directions in the latter. The activation barriers of interconversion were determined to be $13.9 \pm 0.2$ kcal mol$^{-1}$ for (**1**) and $14.6 \pm 0.2$ kcal mol$^{-1}$ for (**2**). The X-ray crystal structures of $[Mo(\eta^3\text{-}C_3H_5)(CO)_2(S_2COEt)(CH_3CN)]$ (**1b**), $[Mo(\eta^3\text{-}C_3H_5)(S_2COEt)(CO)(dppm)]$ (*exo*-**5**), and $[Mo(\eta^3\text{-}C_3H_5)(S_2COEt)(CO)(dppa)]$ (*endo*-, *exo*-**8**) are employed to elucidate the coordination mode of the dithiocarbonate ligand and the *endo*-, *exo*-orientations. One crystallographically independent molecule of **8** is contained in the cell, in which the open face of the allyl group is disordered toward two directions, i.e. endo and *exo*. In addition, the *endo*:*exo* ratio in the solid state is 62:38.



## 1. Introduction

The X-ray crystallography [1] and fluxionality [2] of complexes containing the $[Mo(\eta^3\text{-allyl})(CO)_2(\eta^2\text{-L})X]$ (L: pyrazolylborate, β-diketonate, dithiocarbamate, X: neutral monodentate ligand; L: diphos, pyridylphosphane, X: halide) type have been well studied as an intramolecular trigonal twist. The most important result is that, the coordinated $\eta^3$-allyl group showed a conformation that the open face of the allyl group and the two carbonyl groups are toward in the same direction. An electronic stabilization [3] for this particular orientation is indicated. A pivoted double switch [4] and pyridyl-exchange mechanism have been reported when the L ligands were replacement by pyridylphosphane or their oxides ligands. Notably, the rotational behavior and stereoisomers of complexes with the type $[Mo(\eta^3\text{-allyl})(CO)(PP)(SS)]$ have been studied rarely.

We have previously studied the first *endo*-, *exo*- complexes $[Mo(\eta^3\text{-}C_3H_5)(CO)(dppm)\{S_2P(OEt)_2\}]$ from $^{31}P\{^1H\}$ NMR spectra [5], fluxional behavior and clear crystal structures of two conformations of complexes including the $[Mo(\eta^3\text{-}C_3H_5)(PP)(CO)(SS)]$ type (PP: diphos; SS: dithiocarbamate) [6].

In this work we continuously investigate the syntheses, fluxional behavior and *endo*-, *exo*- conformational crystal structures of *O*-ethyldithiocarbonate Mo(II) complexes. The crystallographic evidences for *endo*- and *exo*-allyl ligand are presented.

* Corresponding author. Tel.: +886 4 26318652x1200; fax: +886 4 26310579.
*E-mail address:* khyih@sunrise.hk.edu.tw (K.-H. Yih).

0022-328X/$ - see front matter © 2008 Elsevier B.V. All rights reserved.
doi:10.1016/j.jorganchem.2008.07.025

## 2. Results and discussion

### 2.1. Syntheses

We have reported a convenient way to prepare the dithio allyl complexes with the type $[Mo(\eta^3\text{-}C_3H_5)(CO)_2(L)]$ ($L = S_2CNC_4H_8$ [7]; $S_2CNEt_2$; $S_2P(OEt)_2$, $CH_3CN$ [8]) from the reaction of complex $[Mo(\eta^3\text{-}C_3H_5)(CO)_2(CH_3CN)_2(Br)]$ and the dithio ligands in acetonitrile at room temperature. Thus, treatment of $[Mo(\eta^3\text{-}C_3H_5)(CO)_2(CH_3CN)_2(Br)]$ with $KS_2COEt$ in methanol at ambient temperature obtained complex $[Mo(CH_3CN)(\eta^3\text{-}C_3H_5)(CO)_2(S_2\text{-}COEt)]$ (**1**) with 90% isolated yield (Scheme 1). Compound **1** is a very air-sensitive red solid which is readily soluble in organic solvents such as dichloromethane, toluene and acetonitrile but insoluble in saturated hydrocarbons. The yellow air-sensitive complex $[Mo(\eta^3\text{-}C_3H_5)(CO)_2(S_2COEt)(C_5H_{10}NH)]$ (**2**) was prepared by the reaction of **1** with $C_5H_{10}NH$ at room temperature with 87% isolated yield. Compound **2** is soluble in polar solvent, and slightly soluble in *n*-hexane. The reaction of **1** and $C_5H_{10}NC(S)SH$ in $CH_2Cl_2$ lead to the clean and high yield formation of the 16-electron dithiocarbamate complex $[Mo(\eta^3\text{-}C_3H_5)(CO)_2(S_2CNC_5H_{10})]$ (**3**) with releasing the EtOC(S)SH ligand. Complex **3** also can be produced from the reaction of **2** with carbon disulfide. The $CS_2$ insertion reaction into the M–N bond (M = Cr, Mo, W) promoted by the abstraction of a proton on the nitrogen atom of the piperidine ligand by $^n$BuLi to form the $\eta^2$-dithiocarbamate ligand have been reported by us [9]. From the reaction, it is believed to be induced by the stronger $\pi$-donor ability of $C_5H_{10}NCS_2^-$ ligand, by insertion of $CS_2$ into the Mo–N bond of **2** to give dithiocarbamate complex **3** with releasing the EtOC(S)SH ligand. The yellow-orange crystalline product **3** was slightly air-sensitive, insoluble in $CH_2Cl_2$, $CH_3CN$ and only slightly soluble in DMSO. Treatment of **1** with bipyridine produced the red air-stable complex $[Mo(\eta^3\text{-}C_3H_5)(bipy)(CO)_2(S_2COEt)]$ (**4**) with 98% isolated yield. Compound **4** also can be obtained from the reaction of **2** with bipy in $CH_2Cl_2$ at room temperature.

Treatment of **1** with various diphos ligands in refluxing acetonitrile yield mixtures of the air-sensitive and yellow-orange complexes $[Mo(\eta^3\text{-}C_3H_5)(CO)(diphos)(S_2COEt)]$ (diphos: dppm, *endo*,

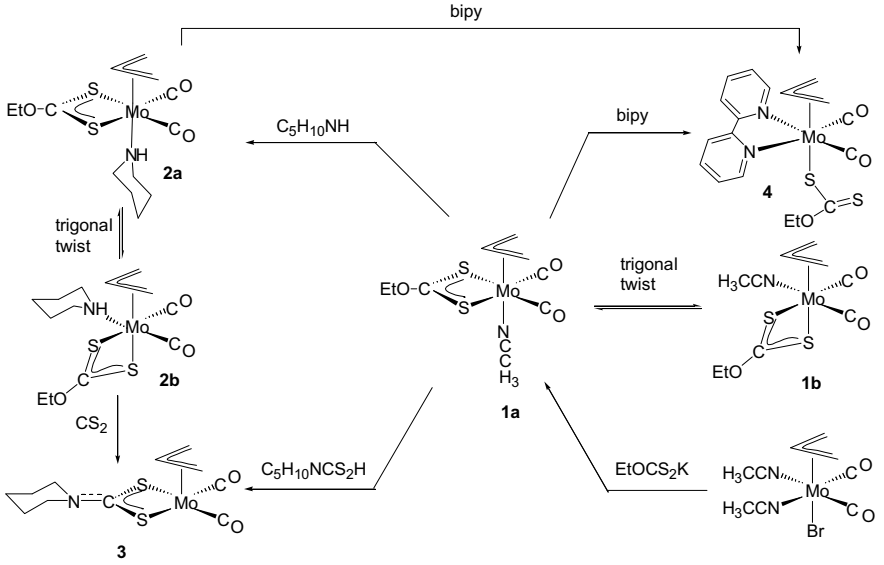


**Scheme 1.**

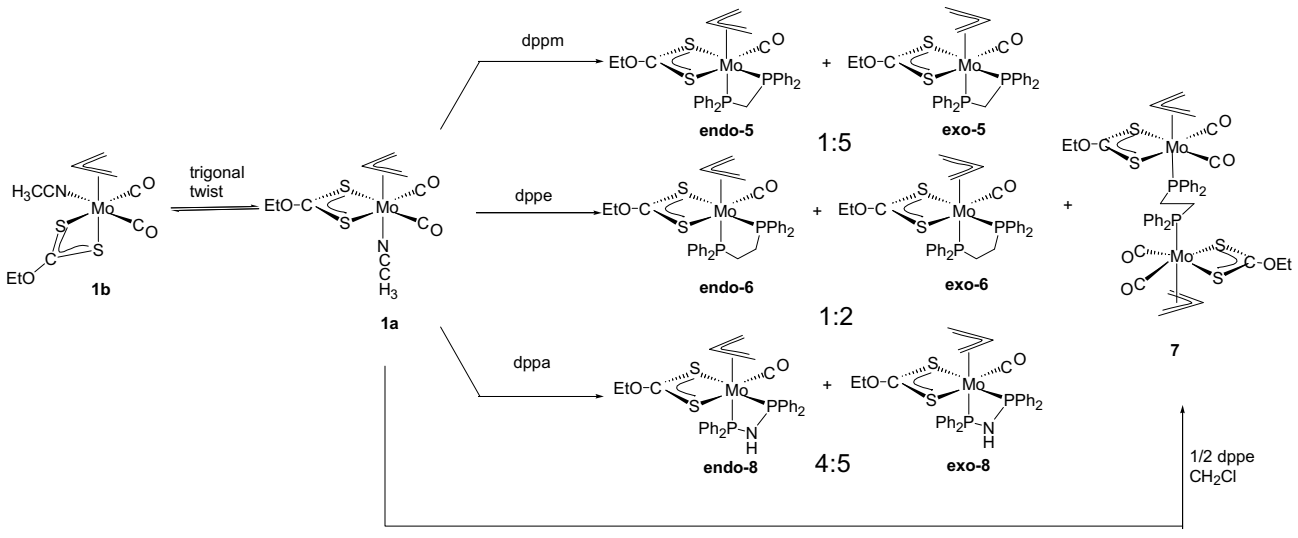


**Scheme 2.**

*exo*-**5**; dppe, *endo*, *exo*-**6**; dppa, *endo*, *exo*-**8**) with *endo*:*exo* ratios of 1:5, 1:2, and 4:5 and *ca.* 88%, 85% and 92% isolated yield, respectively (Scheme 2). The orientations of *endo* and *exo* are defined by the open face of the allyl group and carbonyl group being in the same direction in the former and opposite direction on the latter [6]. Except *endo*, *exo*-**6**, a dimetal complex [Mo($\eta^3$-$C_3H_5$)($S_2$COEt)(CO)]$_2$($\mu$-dppe) (**7**) was obtained in the reaction of **1** and dppe. The $CH_2Cl_2$ solution of dppe was slowly added into a $CH_3CN$ solution of **1** with ratios of 1:2, complex **7** was formed as the sole product with 96% isolated yield.

These compounds **5–8** are soluble in dichloromethane, slightly soluble in acetonitrile and insoluble in diethyl ether and *n*-hexane. The compounds **1**, **2**, **4–8** were already of good purity, but analytically pure samples could be obtained by slow *n*-hexane diffusion into a dichloromethane solution at +4 °C. All characterization data are consistent with the proposed constitution.

### 2.2. IR and MS spectroscopy

The presence of one or two carbonyl groups for all complexes in this work is clearly reflected in the IR spectra. In KBr, two terminal carbonyl-stretching bands were found in equal intensity in **1–4** and **7**; this observation indicates that the two carbonyls are mutually *cis*. Although both isomers are known to be present in different ratios, only one terminal carbonyl-stretching band was found in **5**, **6**, and **8**. Because of limited solubility, all IR spectra needed to be recorded in $CH_2Cl_2$, and therefore any small difference might be obscured by the natural line-broadening in this solvent. In the FAB mass spectra, base peaks with the typical Mo isotope distribution are in agreement with the [$M^+$] molecular ion for complexes **1–7** and [$M^+$−CO] for complex **8**.

### 2.3. NMR spectroscopy

From an $AM_2X_2$ pattern of the allyl group in the $^1$H NMR spectra and one equivalent resonance of the terminal carbon of the allyl group and one resonance of carbonyl group in the $^{13}C\{^1H\}$ NMR spectra, it looks as if **1** has the geometry with a mirror plane through the center carbon of allyl group, Mo, O atom of the dithiocarbamate ligand and $CH_3CN$; i.e., the bidentate ligand and the two carbonyls lie in a horizontal plane, whereas the allyl group and the $CH_3CN$ ligand lie in trans positions above and below the plane, respectively (Fig. 1). Because the mentioned structure is incompatible with the report by Miguel [10], the variable-temperature $^1$H NMR experiments were undertaken. By variable-temperature $^1$H NMR spectra, complex **1** in solution exhibits fluxional behavior, and the dynamic process has been examined. As depicted in Fig. 1, an $AM_2X_2$ pattern is observed for the allyl protons, and a single resonance for the methyl protons of the acetonitrile group. However, on cooling $(CD_3)_2CO$ solutions of **1**, the proton signals initially broaden and below 296 K the methyl resonance of $CH_3CN$ and the *syn*- and *anti*-proton signals of the allyl moiety each begin to separate into two components. Below 223 K, $^1$H NMR data are shown another set of peaks (ABCDX), which is in according with the solid-state geometry of **1b**. The mechanism can be described as a trigonal twist, in which the rotation of the triangular face formed by the $CH_3CN$ and the two sulfur atoms relative to the face formed by the allyl and the two carbonyl groups. The rotation mechanism has been previously described for the trigonal twist behavior of [Mo(pd)($\eta^3$-$C_3H_5$)(CO)$_2$(py)] [11] and other related complexes [12]. Line-shaped analysis of the variable-temperature has been calculated from $^1$H NMR spectra of **1** yields a value of 13.9 ± 0.2 kcal mol$^{-1}$ for $\Delta G^{\ddagger}$. Compared with other trigonal twist complexes, the activation energy of **1** is larger than those of complex Mo($\eta^3$-$C_3H_5$)(CO)$_2$(dppm)I (11.2 kcal mol$^{-1}$) [13] and [Mo($\eta^3$-$C_3H_5$)(CO)$_2${($S_2$P(OEt)$_2$)}($CH_3CN$)] (11.6 kcal mol$^{-1}$) [8] and is smaller than that of complex [Mo(pd)($\eta^3$-$C_3H_5$)(CO)$_2$(py)] (14.3 kcal mol$^{-1}$) [10].

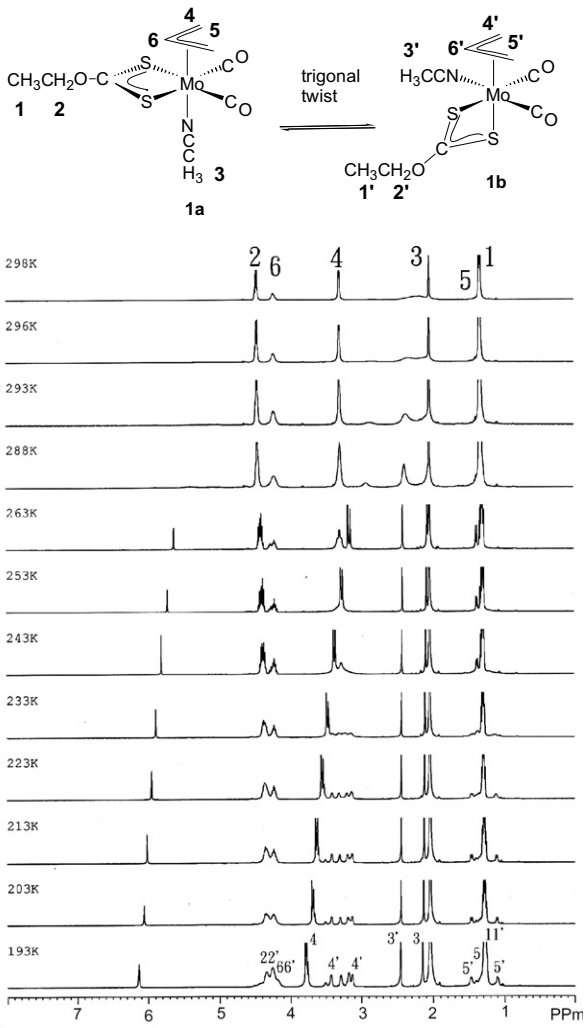


**Fig. 1.** Variable-temperature $^1$H NMR spectra of **1** in acetone-$d_6$.

Similar spectroscopic phenomena of the carbonyl group and allyl moiety in IR and $^1$H, $^{13}C\{^1H\}$ NMR spectra guide us to believe that complex **2** contains the same solution rotational behavior as **1**. To confirm the result, the variable-temperature $^1$H NMR experiments of **2** were carried out. $\Delta G^{\ddagger}$ value calculated from line-shape analysis of the variable-temperature $^1$H NMR is 14.6 ± 0.2 kcal mol$^{-1}$ for **2**. The large activation energy of **2** compared with **1** is due to the more steric hindrance of the $C_5H_{10}NH$ ligand than $CH_3CN$. In fact, this value is essentially independent of the nature of dithiocarbonato ligand, increases with increase in the size of the neutral monodentate ligand, and greater for the substitute allyl than for the allyl complexes. Notably, the dissociation mechanism [10] of the $C_5H_{10}NH$ ligand was neglected because increasing the temperature to 330 K resolved no signals of free $C_5H_{10}NH$.

The $^1$H and $^{13}C\{^1H\}$ NMR spectral data of **3** are the same as those of the known 16 electron complex [Mo($\eta^3$-$C_3H_5$)(CO)$_2$-($S_2CNC_5H_{10}$)] [8]. From an $AM_2X_2$ pattern of the allyl group in the $^1$H NMR spectra and one equivalent resonance of the terminal carbon of the allyl group, four sets resonance of bipyridine group, and one resonance of carbonyl group in the $^{13}C\{^1H\}$ NMR spectra, the geometry of **4** was shown a mirror plane through the center carbon of allyl group, Mo, and coordinative S atom of the dithiocarbonato ligand; i.e., the bipyridine ligand and the two carbonyls lie in a

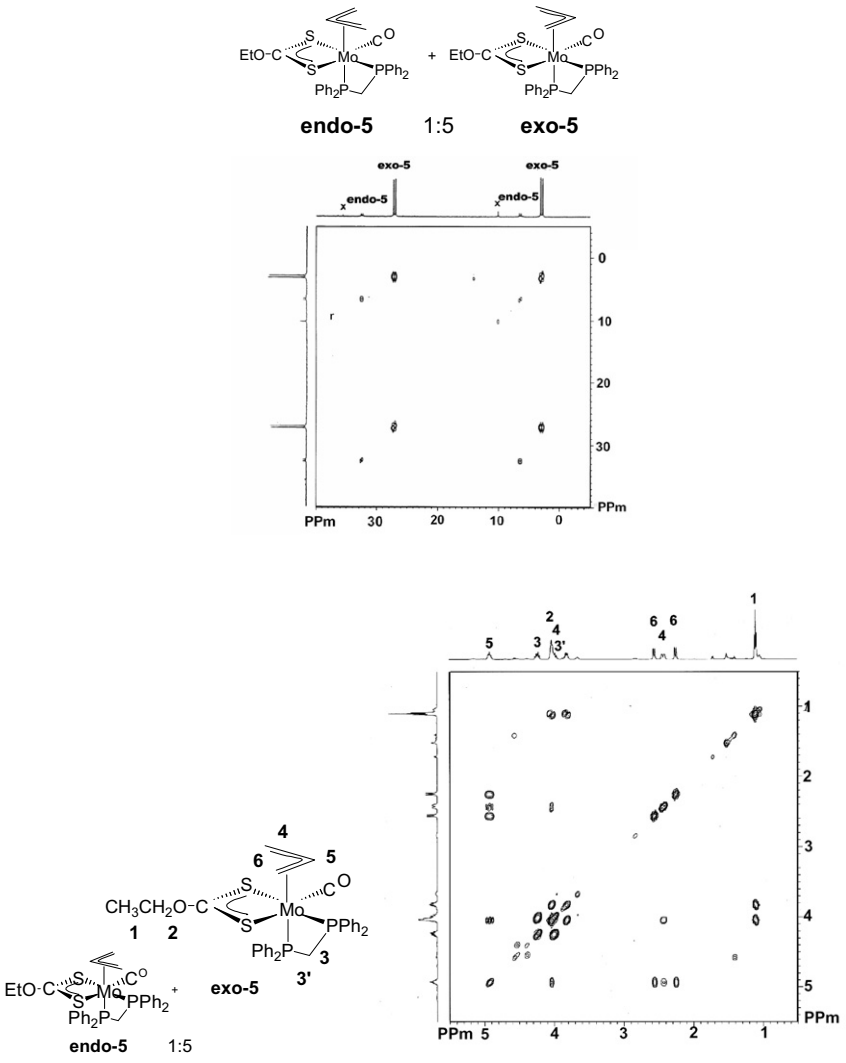


**Fig. 2.** (a) Homonuclear shift-correlated 2-D NMR spectrum for $^{31}P$ nuclei with $^{1}H$ decoupling for the mixtures *endo*-**5** and *exo*-**5** in acetone-$d_6$. (b) Homonuclear shift-correlated 2-D NMR spectrum of *endo*- and *exo*-**5** (1:5) in $CDCl_3$.

**Table 1**
Crystal data and refinement details for complexes **1b**, *exo*-**5**, and *endo*, *exo*-**8**

| | **1b** | *exo*-**5** | *endo*, *exo*-**8** |
|---|---|---|---|
| Chemical formula | $C_{10}H_{13}NO_3S_2Mo$ | $C_{32}H_{32}O_2P_2S_2Mo$ | $C_{31}H_{31}NO_2P_2S_2Mo$ |
| Formula weight | 355.27 | 670.58 | 671.57 |
| Crystal system | Monoclinic | Monoclinic | Monoclinic |
| Space group | $P2_1/c$ | $P2_1$ | $P2_1/n$ |
| $a$ (Å) | 7.2178(1) | 10.2519(2) | 12.7835(2) |
| $b$ (Å) | 12.2401(2) | 15.8528(2) | 14.5988(2) |
| $c$ (Å) | 16.1978(3) | 11.7698(2) | 16.4824(2) |
| $\alpha$ (°) | 90 | 90 | 90 |
| $\beta$ (°) | 100.394(1) | 103.0812(9) | 94.2263(7) |
| $\gamma$ (°) | 90 | 90 | 90 |
| $V$ (Å$^3$) | 1407.54(4) | 1510.61(5) | 3067.64(7) |
| $Z$ | 4 | 2 | 4 |
| $\rho_{calcd}$ (g cm$^{-3}$) | 1.677 | 1.474 | 1.454 |
| $\mu$ (Mo K$\alpha$) (mm$^{-1}$) | 1.223 | 0.707 | 0.697 |
| $\lambda$ (Å) | 0.71073 | 0.71073 | 0.71073 |
| $T$ (K) | 150(1) | 150(1) | 150(1) |
| $\theta$ Range (°) | 2.10–27.50 | 1.78–27.50 | 2.12–27.50 |
| Independent reflections | 3231 | 6668 | 7043 |
| Number of variables | 156 | 353 | 372 |
| $R$[a] | 0.017 | 0.036 | 0.035 |
| $R_w$ | 0.044 | 0.076 | 0.078 |
| $S$[b] | 1.057 | 1.039 | 1.045 |

[a] $R = \sum||F_o| - |F_c||/\sum|F_o|$.
[b] Quality-of-fit = $[\sum w(|F_o| - |F_c|)^2/(N_{observed} - N_{parameters})]^{1/2}$.

horizontal plane, whereas the allyl group and the dithiocarbonato ligand lie in trans positions above and below the plane, respectively (Scheme 1). Variable temperature (183–298 K) $^1$H NMR experiments were used to confirm no intramolecular trigonal twist behavior in complex **4** due to the steric hindrance of bipyridine and dithiocarbonato ligands.

The $^1$H and $^{13}$C{$^1$H} NMR spectral data for complex [Mo($\eta^3$-$C_3H_5$)($S_2$COEt)(CO)(dppm)] (**5**) are obtained only for the major products, because of the low ratio and no isolation of the minor products. Interestingly, their room temperature $^1$H NMR spectra (Fig. 2) exhibit five sets of resonances for the allyl moiety typical of the ABCDX spin patterns of unsymmetrical $\eta^3$-allyl dithiocarbonate metal complexes.

In the $^1$H NMR spectrum of *exo*-**5**, the methylene protons of the dppm ligand and allyl protons exhibit seven equally intense resonances at $\delta$ 3.82, 4.22 and at $\delta$ 2.24, 2.55 (H*anti*), $\delta$ 2.42, 4.01 (H*syn*), $\delta$ 4.91 (H*center*), respectively. The corresponding $^{13}$C{$^1$H} NMR signals are at $\delta$ 41.5, and $\delta$ 54.7, 68.9, 100.6. In the $^{13}$C{$^1$H} NMR spectrum of *exo*-**5**, two resonances appear in the carbonyl region. One resonance at $\delta$ 227.1 is attributed to the carbonyl group and the resonance at $\delta$ 222.5 is assigned to the carbon atom of the $CS_2$ of the $EtOCS_2$ ligand. The other $^1$H and $^{13}$C{$^1$H} NMR spectra of complexes **6** and **8** are similar to that of **5**.

Compared to the $^{31}$P{$^1$H} NMR spectra and the structures of the complexes *exo*-**5**, and *endo*-, *exo*-**8**, it can be concluded that: (1) the dithiocarbonate ligand improves the formation of *exo*-products; (2) *exo*-complexes show larger $J_{P-P}$ coupling constants than those of *endo*-complexes; (3) the resonances of dppm, dppe and dppa complexes appear in relative up-field for the *exo*-orientation.

A rearrangement involving a π–σ–π [14] process or allyl rotation or intramolecular trigonal twist rearrangement have been reported in [Mo($\eta^3$-allyl)] type complexes. In the range of 298–348 K, the variable-temperature $^1$H and $^{31}$P{$^1$H} NMR experiments were undertaken to investigate the interconversion of complexes *endo*, *exo*-**5** and *endo*, *exo*-**8**. Because these complexes were decomposed in $CDCl_3$ at higher temperatures and poorly soluble in $CD_3CN$, these measurements were not pursued further.

### 2.4. X-ray single-crystal structures of *1b*, endo-*5*, and endo-, exo-*8*

For satisfactory structural characterization, we performed X-ray diffraction studies of **1b**, *endo*-**5**, and *endo*-, *exo*-**8** to elucidate the unequivalent allyl group and *endo*- and *exo*-conformers at 150 K. Crystal data and refinement details and selected interatomic distances (Å) and angles (°) of complexes **1b**, *endo*-**5**, and *endo*-, *exo*-**8** are listed in Tables 1 and 2, respectively. ORTEP plots of the three complexes are shown in Figs. 3–5.

An ORTEP plot of **1b** is shown in Fig. 3. The coordination geometry around the molybdenum atom is approximately an octahedron with the two *O*-ethyldithiocarbonato sulfur atoms, acetonitrile, two carbonyls and the allyl group occupying the six coordination sites. The structure confirms an asymmetric allyl group. One of the sulfur atoms of dithiocarbonato is *trans* to the allyl: S(2)–Mo–C(4), 157.88(4)°, while the other is *trans* to one carbonyl: S(1)–Mo–C(2), 162.93(5)°. The remaining carbonyl is *trans* to the nitrogen atom of the acetonitrile: C(1)–Mo–N(1), 168.14(5)°. The S–Mo–S angle of 68.87(11)° in **1b** is similar to 68.53(3)° in **5** and 68.04(2)° in **8** within the experimental errors. The Mo–C(3), C(4) and C(5) bond distances are 2.324(2), 2.221(2) and 2.332(2) Å, respectively. The Mo–S(2) distance of 2.5350(4) Å (*trans* to allyl) is clearly shorter than Mo–S(1) of 2.6167(4) Å (*trans* to CO) because of the higher *trans* influence induced by the CO group more than the allyl group.

From Figs. 4 and 5, the open face of the allyl group is oriented towards the carbonyl group in *endo*-**8** and in the opposite directions in *exo*-**5** and ***exo*-8**. In the three structures, the coordination

**Table 2**
Selected interatomic distances (Å) and angles (°) for **1b**, *exo*-**5**, and *endo*, *exo*-**8**

| Bond lengths | | Bond angles | |
|---|---|---|---|
| *Compound **1b*** | | | |
| Mo–C(1) | 1.9518(14) | C(1)–Mo–C(2) | 78.48(6) |
| Mo–C(2) | 1.9595(15) | C(1)–Mo–N(1) | 168.14(5) |
| Mo–C(3) | 2.324(2) | C(2)–Mo–S(2) | 94.26(5) |
| Mo–C(4) | 2.2214(15) | C(4)–Mo–S(2) | 157.88(4) |
| Mo–C(5) | 2.3382(15) | C(1)–Mo–C(4) | 105.25(6) |
| Mo–N(1) | 2.2394(12) | C(2)–Mo–S(1) | 162.93(5) |
| Mo–S(1) | 2.6167(4) | S(1)–Mo–S(2) | 68.870(11) |
| Mo–S(2) | 2.5350(4) | C(3)–C(4)–C(5) | 115.90(14) |
| C(3)–C(4) | 1.415(2) | S(1)–C(6)–S(2) | 118.41(8) |
| C(4)–C(5) | 1.412(2) | N(1)–C(9)–C(10) | 179.6(2) |
| *Compound exo-**5*** | | | |
| Mo–C(1) | 1.912(3) | C(3)–Mo–P(1) | 163.84(14) |
| Mo–C(3) | 2.328(4) | P(2)–Mo–P(1) | 67.44(3) |
| Mo–C(4) | 2.341(4) | C(1)–Mo–S(1) | 99.79(10) |
| Mo–C(2) | 2.357(4) | P(2)–Mo–S(1) | 141.77(4) |
| Mo–P(2) | 2.4490(9) | P(1)–Mo–S(1) | 77.83(3 |
| Mo–P(1) | 2.4697(9) | C(1)–Mo–S(2) | 167.89(10) |
| Mo–S(1) | 2.5157(7) | C(2)–Mo–S(2) | 88.91(11) |
| Mo–S(2) | 2.6102(9) | P(2)–Mo–S(2) | 94.75(3) |
| S(1)–C(5) | 1.679(4) | S(1)–Mo–S(2) | 68.53(3) |
| S(2)–C(5) | 1.694(4) | O(1)–C(1)–Mo | 179.0(3) |
| O(1)–C(1) | 1.179(4) | C(4)–C(3)–C(2) | 121.5(5) |
| C(2)–C(3) | 1.371(7) | | |
| C(3)–C(4) | 1.365(7) | | |
| *Compound endo, exo-**8*** | | | |
| Mo–C(1) | 1.915(3) | C(1)–Mo–C(3′) | 81.6(5) |
| Mo–C(3′) | 2.217(8) | C(1)–Mo–C(3) | 102.2(3) |
| Mo–C(3) | 2.306(5) | C(3′)–Mo–C(4) | 27.8(3) |
| Mo–C(4′) | 2.315(9) | C(3)–Mo–C(4) | 34.1(3) |
| Mo–C(2) | 2.318(3) | C(1)–Mo–P(1) | 85.07(9) |
| Mo–C(4) | 2.401(5) | C(4′)–Mo–C(2) | 62.0(3) |
| Mo–P(1) | 2.4212(7) | C(2)–Mo–C(4) | 61.96(19) |
| Mo–P(2) | 2.4662(7) | C(4′)–Mo–P(2) | 156.0(3) |
| Mo–S(1) | 2.5156(8) | C(4)–Mo–P(2) | 153.67(19) |
| Mo–S(2) | 2.6053(7) | P(1)–Mo–P(2) | 65.57(2) |
| S(1)–C(5) | 1.704(3) | S(1)–Mo–S(2) | 68.04(2) |
| S(2)–C(5) | 1.676(3) | N(1)–P(1)–Mo | 96.09(8) |
| P(1)–N(1) | 1.691(2) | N(1)–P(2)–Mo | 94.80(8) |
| P(2)–N(1) | 1.678(2) | P(2)–N(1)–P(1) | 103.53(12) |
| O(1–)C(1) | 1.181(4) | O(1)–C(1)–Mo | 179.0(3) |
| C(2)–C(3′) | 1.360(14) | C(4)–C(3)–C(2) | 121.1(9) |
| C(2)–C(3) | 1.408(8) | C(4′)–C(3)–C(2) | 123.2(17) |
| C(3)–C(4) | 1.382(13) | C(3′)–C(4′)–Mo | 68.7(5) |
| C(3′)–C(4′) | 1.35(2) | S(2)–C(5)–S(1) | 115.96(16) |

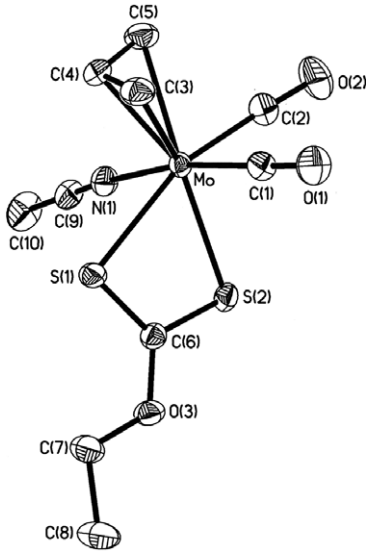


**Fig. 3.** An ORTEP drawing with 50% thermal ellipsoids and atom-numbering scheme for the complex [Mo($CH_3CN$)($\eta^3$-$C_3H_5$)(CO)$_2$($\eta^2$-$S_2$COEt)] (**1b**).

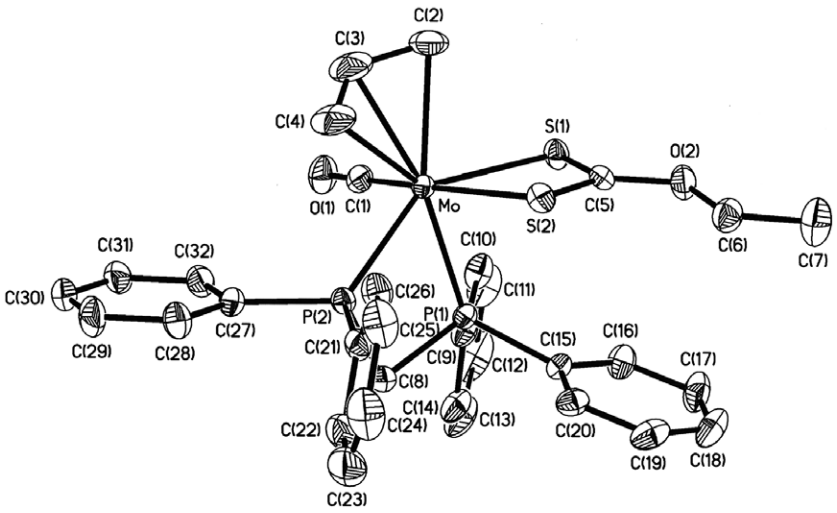


**Fig. 4.** An ORTEP drawing with 50% thermal ellipsoids and atom-numbering scheme for the complex [Mo($\eta^2$-dppm)($\eta^3$-$C_3H_5$)(CO)($\eta^2$-$S_2$COEt)] (*exo*-**5**).

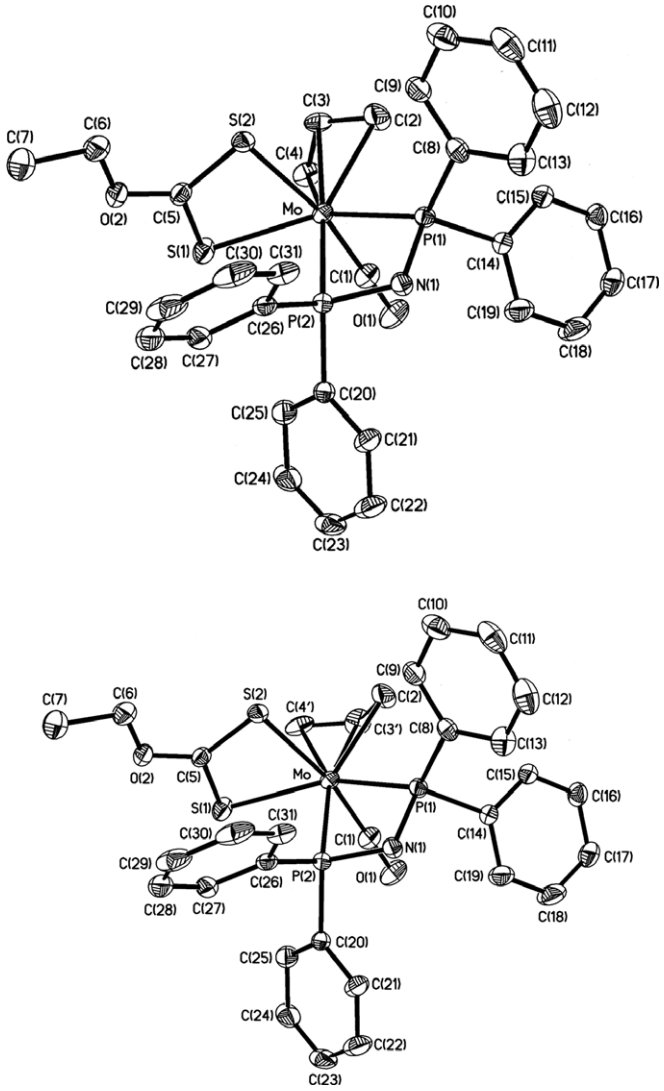





**Fig. 5.** ORTEP drawing with 30% thermal ellipsoids and atom-numbering scheme for the complex [Mo($\eta^2$-dppa)($\eta^3$-$C_3H_5$)(CO)($\eta^2$-$S_2$COEt)] (*endo*, *exo*-**8**).

geometry around the molybdenum atom is approximately an octahedron with the two sulfur atoms of the dithiocarbonato ligand, two phosphorus atoms of the diphos ligand, one carbonyl and the allyl group occupying the six coordination sites. It is confirmed that the allyl groups in three structures are asymmetric. One of the sulfur atoms of dithiocarbonato ligand is *trans* to the diphos: S–Mo–P, 141.77(4)–144.40(3)°, while the other is *trans* to carbonyl: S–Mo–C, 167.89(10)–169.39(9)°. The S(1)–Mo–S(2) angles 68.04(2)–68.53(3)° in dithiocarbonate complexes are similar to 68.071(17)–68.459(17)° in dithiocarbamate complexes and smaller than 75.27(57)–76.02(5)° in dithiophosphate complexes [6] because of the different $PS_2$ and $CS_2$ hybridization of the P and C atoms. An examination of the S(1)–C(5)–S(2) bond distances and angles shows a geometrical environment characteristic of a $sp^2$ hybridization of the carbon atom. In addition, the S(1)–C(5)–S(2) angles in the range of 115.96(16)–117.72(19)°, are significantly different from the S(1)–P–S(2) angles which are in the range of 109.67(10)–111.07(10)°.

The short C–OEt bond length 1.321(2) –1.341(4) Å of the dithiocarbonate complexes **1b** *endo*-**5**, and *endo*-, *exo*-**8** indicate a considerable partial double bond character (C–O: 1.43, C=O: 1.20, C≡O: 1.128 Å). The Mo–S(1) distance (*trans* to phosphorus) is clearly shorter than Mo–S(2) (*trans* to CO) because of the higher *trans* influence induced by the CO group more than the phosphine group. Similarly, the Mo–P distance (*trans* to sulfur) is slightly shorter than Mo–P (*trans* to allyl) because of the higher *trans* influence induced by the allyl group more than the dithiocarbonato group. The Mo–S (2.5156(8)–2.6167(4) Å) and Mo-allyl (2.217(8)–2.401(5) Å) bond distances are consistent with the values reported for $Mo^{II}$–S and numerous Mo-allyl systems [1a,2,15]. The bond distances and intercarbon angle of allyl group in complexes **1b**, *endo*-**5**, and *endo*-, *exo*-**8** (1.412(2)–1.415(2) Å, 1.365(7)–1.371(7) Å, 1.35(2)–1.408(8) Å and 115.90(14)–123.2(17)°) are insignificantly different and close to the region of related $Mo^{II}$-allylic compounds (1.31–1.42 Å, 115–125°) [13]. The Mo–P bond lengths are in the region of 2.4212(7)–2.4697(9) Å, and appear to be normal. The carbonyl ligand is essentially linear with region of 174.98(13)–179.0(3)°. The values for the Mo–CO angles are similar to those found for other terminal carbonyls contained in Mo systems. The Mo–CO (1.912(3)–1.9595(15) Å) and C–O distances are both within the range of values reported for other molybdenum carbonyl complexes [4,5,8,15].

X-ray structure determination of **8** at 150 K reveals the presence of two crystallographically inequivalent molecules in the nuit cell,

which differ mainly by the orientation of the allyl group with respect to the carbonyl group. The two molecules *endo*-**8** and *exo*-**8** with ratio of 1:1 were depicted in Fig. 5 together with the labeling scheme. The ratio of *endo*-**8**:*exo*-**8** is 62:38 in solid state and with 4:5 ratio in solution state by integrating from $^{31}P\{^1H\}$ NMR spectra. To our knowledge, the concomitant presence of two different allyl orientation isomers of this kind in one unit cell has been rarely noted [16].

## 3. Concluding remarks

The trigonal twist fluxional behavior of the *O*-ethyldithiocarbonate Mo complexes **1** and **2** were confirmed and the activation barriers of interconversion were determined to be 13.9 ± 0.2 kcal mol$^{-1}$ and 14.6 ± 0.2 kcal mol$^{-1}$, respectively. We employ three different diphos ligands to investigate the dependence of the ratio of the *endo*- and *exo*-conformer. The *O*-ethyldithiocarbonato ligand improves the formation of *exo*-products in the three diphos ligands, whereas it is different to the previous report that the dithiophosphate ligand improves the formation of *endo*-products and the dithiocarbamate ligands improve the formation of *endo*-products in dppe ligand and of *exo*-products in dppm ligand. The *exo*-complexes show larger $J_{P-P}$ coupling constants than *endo*-complexes and the resonances of dppm, dppe and dppa complexes appear in relative up-field for the *exo*-orientation. These results are identical with the dithiocarbamate and dithiophosphate ligands. The X-ray crystal structures of [Mo($\eta^3$-$C_3H_5$)(CO)$_2$($S_2$COEt)($CH_3CN$)] (**1**), [Mo($\eta^3$-$C_3H_5$)($S_2$COEt)(CO)(dppm)] (*exo*-**5**), and [Mo($\eta^3$-$C_3H_5$)($S_2$COEt)(CO)(dppa)] (*endo*-, *exo*-**8**) are employed to elucidate the coordination mode of the *O*-ethyldithiocarbonato ligand and the *endo*-, *exo*-orientations.

## 4. Experimental

### 4.1. General procedures

All manipulations were performed under nitrogen using vacuum-line, drybox, and standard Schlenk techniques. NMR spectra were recorded on a Bruker AM-200, or on an AM-500 WB FT-NMR spectrometer and are reported in units of parts per million with residual protons in the solvent as an internal standard ($CDCl_3$, $\delta$ 7.24; $CD_3CN$, $\delta$ 1.93; $C_2D_6CO$, $\delta$ 2.04). IR spectra were measured on a Nicolet Avatar-320 instrument and referenced to polystyrene standard, using cells equipped with calcium fluoride windows. MS spectra were recorded on a JEOL SX-102A spectrometer. Solvents were dried and deoxygenated by refluxing over the appropriate reagents before use. *n*-Hexane, diethyl ether, THF and benzene were distilled from sodium-benzophenone. Acetonitrile and dichloromethane were distilled from calcium hydride, and methanol was distilled from magnesium. All other solvents and reagents were of reagent grade and used as received. Elemental analyses and X-ray diffraction studies were carried out at the Regional Center of Analytical Instrument located at the National Taiwan University. $Mo(CO)_6$ and $C_3H_5Br$ were purchased from Strem Chemical, $EtOCS_2K$, dppm, dppe, and dppa, were purchased from Merck.

### 4.2. Preparation of **1**

MeOH (20 ml) was added to a flask (100 ml) containing a mixture of $EtOCS_2K$ (0.160 g, 1.0 mmol) and [Mo($CH_3CN$)$_2$($\eta^3$-$C_3H_5$)(CO)$_2$(Br)] [17] (0.317 g, 1.0 mmol). The solution was stirred for 10 min, and an IR spectrum indicated completion of the reaction. After removal of the solvent in vacuo, the residue was redissolved with $CH_2Cl_2$ (10 ml). *n*-Hexane (25 ml) was added to the solution and a red solids **1** were formed which were isolated by filtration (G4), washed with *n*-hexane (2 × 10 ml) and subsequently drying under vacuum yielding a mixture of [Mo($CH_3CN$)($\eta^3$-$C_3H_5$)(CO)$_2$($S_2$COEt)] (**1**) (0.32 g, 90%) as a red microcrystalline solid. Further purification was accomplished by recrystallization from 1/10 $CH_2Cl_2$/*n*-hexane. Spectroscopic data of **1** are as follows. IR (KBr, $\upsilon_{CO}$/cm$^{-1}$): 1935(vs), 1860(vs). $^1H$ NMR (500 MHz, $C_3D_6O$, 298 K): $\delta$ 1.33 (t, 3H, $OCH_2CH_3$, $J_{H-H}$ = 11.6 Hz), 1.35 (m, 2H, H*anti*), 2.05 (br, 3H, $CH_3CN$), 3.29 (d, 2H, H*syn*, $J_{H-H}$ = 10.8 Hz), 4.22 (m, 1H, H*centre*), 4.46 (q, 2H, $OCH_2$, $J_{H-H}$ = 11.6 Hz). $^{13}C\{^1H\}$ NMR (125 MHz, $C_3D_6O$, 298 K): $\delta$ 0.9 (s, $CH_3CN$), 13.1 (s, $OCH_2CH_3$), 56.4 (br, $CH_2$=CH), 67.7 (s, $OCH_2$), 73.2 (br, $CH_2$=CH), 116.2 (s, $CH_3CN$), 227.2 (s, CO). Anal. Calc. for $C_{10}H_{13}NO_3S_2Mo$: C, 26.01; H, 2.84; N, 3.03. Found: C, 26.25; H, 2.91; N, 3.02%.

### 4.3. Preparation of **2**

A solution of [Mo($CH_3CN$)($\eta^3$-$C_3H_5$)(CO)$_2$($S_2$COEt)] (**1**) (0.355 g, 1.0 mmol) in $CH_2Cl_2$ (20 ml) was treated with $C_5H_{10}NH$ (0.1 ml, 1.2 mmol) at ambient temperature. Instantly, the reaction mixture turned to yellow. After 10 min of stirring, the solution was dried in vacuo. Subsequently, *n*-hexane (40 ml) was added to the solution and a yellow precipitate was formed. The precipitate was collected by filtration (G4) and dried in vacuo to yield 0.35 g (87%) of [Mo($\eta^3$-$C_3H_5$)(CO)$_2$($S_2$COEt)($C_5H_{10}NH$)] (**2**). IR (KBr, cm$^{-1}$): $\upsilon$(CO) 1929(vs), 1836(vs) cm$^{-1}$. $^1H$ NMR (500 MHz, $CDCl_3$, 298 K): $\delta$ 1.12 (d, 2H, H*anti*, $J_{H-H}$ = 9.4 Hz), 1.33 (t, 6H, $OCH_2CH_3$, $J_{H-H}$ = 7.4 Hz), 1.77 (m, 6H, $NCH_2CH_2CH_2$), 3.25 (d, 2H, H*syn*, $J_{H-H}$ = 6.6 Hz), 3.53 (m, 4H, $NCH_2$), 3.90 (m, 1H, C*centre*), 4.08 (q, 4H, $OCH_2$, $J_{H-H}$ = 7.4 Hz). $^{13}C\{^1H\}$ NMR (125 MHz, $CDCl_3$, 298 K): $\delta$ 16.0 (s, $OCH_2CH_3$), 25.6 (s, $NCH_2CH_2CH_2$), 49.9 (s, $NCH_2CH_2$), 56.0 (s, CH=$CH_2$), 63.0 (s, $NCH_2$), 64.0 (s, $OCH_2$), 72.0 (s, $CH_2$=CH), 195.1 (s, $OCS_2$), 219.6 (s, CO). MS (FAB, NBA): *m/z* 399 ($M^+$). Anal. Calc. for $C_{13}H_{21}NO_3S_2Mo$: C, 39.09; H, 5.30; N, 3.51. Found: C, 39.25; H, 5.61; N, 3.42%.

### 4.4. Preparation of **3**

*Method A: A solution of $C_5H_{10}NC(S)SH$ (0.161 g, 1.0 mmol) in MeOH (5 ml) was added to a flask containing* **1** (0.355 g, 1.0 mmol) in $CH_2Cl_2$ (20 ml). The solution was stirred for 1 min and a yellow-orange precipitate formed. The precipitate was collected by filtration (G4), washed with *n*-hexane (2 × 10 ml) and then dried in vacuo to yield 0.35 g (99%) of **3**. IR (KBr) $\upsilon$(CO) 1945(vs), 1917(vs), 1865(vs), 1847(vs) cm$^{-1}$. $^1H$ NMR (200 MHz, DMSO-$d_6$, 298 K): $\delta$ 1.17 (d, 2H, H*anti*, $J_{H-H}$ = 9.8 Hz), 1.50 (m, 6H, $NCH_2CH_2CH_2$), 3.13 (d, 2H, H*syn*, $J_{H-H}$ = 6.4 Hz), 3.83 (m, 4H, $NCH_2$), 4.00 (m, 1H, CH of allyl). $^{13}C\{^1H\}$ NMR (50 MHz, DMSO-$d_6$, 298K): $\delta$ 23.7 (s, $NCH_2CH_2CH_2$), 25.7 (s, $NCH_2CH_2$), 48.0 (s, $NCH_2$), 58.1 (s, CH=$CH_2$), 74.7 (s, $CH_2$=CH), 204.2 (s, $CS_2$), 230.1 (s, CO). MS (EI, 20 eV): *m/z* 355 ($M^+$), 327 ($M^+$−CO), 299 ($M^+$−2CO). Anal. Calc. for $C_{11}H_{15}NO_2S_2Mo$: C, 37.39; H, 4.28; N, 3.97. Found: C, 37.52; H, 4.42; N, 3.75%.

*Method B: An aliquot of $CS_2$ (0.1 ml, 1.6 mmol) was added to a solution of* **2** (0.399 g, 1.0 mmol) in $CH_2Cl_2$ (20 ml). Instantly, the reaction is completely. A yellow-orange precipitate was formed which was isolated by filtration (G4), and was washed with *n*-hexane (2 × 10 ml) and subsequently dried under vacuum to yield 0.33 g (94%) of **3**.

### 4.5. Preparation of **4**

MeOH (20 ml) was added to a flask (100 ml) containing a mixture of bipy (0.228 g, 1.0 mmol) and [Mo($CH_3CN$)($\eta^3$-$C_3H_5$)(CO)$_2$($S_2$COEt)] (**1**) (0.355 g, 1.0 mmol) at ambient temperature. Instantly, the reaction mixture turned to red and a red precipitate was formed. The precipitate was collected by filtration

(G4) and dried in vacuo to yield 0.46 g (98%) of [Mo($\eta^3$-$C_3H_5$)(CO)$_2$($S_2$COEt)(bipy)] (**4**). Spectroscopic data of **4** are as follows. IR (KBr, cm$^{-1}$): $\upsilon$(CO) 1932(vs), 1858(vs). $^1$H NMR (500 MHz, $CDCl_3$, 298 K): δ 1.52 (d, 2H, H*anti*, $J_{H-H}$ = 4.74 Hz), 1.62 (t, 3H, $OCH_2CH_3$, $J_{H-H}$ = 7.12 Hz), 2.94 (m, 1H, H*c*), 3.03 (d, 2H, H*syn*, $J_{H-H}$ = 5.83 Hz), 4.77 (q, 2H, $OCH_2$, $J_{H-H}$ = 7.12 Hz), 7.41 (d, 2H, $H_1$ of bipy, $J_{H-H}$ = 6.49 Hz), 7.91 (t, 2H, $H_2$ of bipy, $J_{H-H}$ = 7.43 Hz), 8.03 (t, 2H, $H_3$ of bipy, $J_{H-H}$ = 8.18 Hz), 8.70 (d, 2H, $H_4$ of bipy, $J_{H-H}$ = 5.20 Hz). $^{13}$C{$^1$H} NMR (125 MHz, $CDCl_3$, 298 K): δ 14.0 (s, $OCH_2CH_3$), 55.3 (s, $OCH_2$), 70.5 (s, CH=$CH_2$), 75.9 (s, $CH_2$=CH), 122.0, 126.1, 138.0, 152.6 (s, C of bipy), 224.9 (s, $CS_2$), 227.6 (s, CO). MS (FAB, NBA, *m/z*) 471 ($M^+$), 430 ($M^+-C_3H_5$). Anal. Calc. for $C_{18}H_{18}N_2O_3S_2Mo$: C, 45.95; H, 3.86 ; N, 5.96. Found: C, 46.05; H, 3.95; N, 5.52%.

### 4.6. Preparation of endo-, exo-**5**

MeCN (20 ml) was added to a flask (100 ml) containing a mixture of dppm (0.384 g, 1.0 mmol) and [Mo($CH_3CN$)($\eta^3$-$C_3H_5$)(CO)$_2$($S_2$COEt)] (**1**) (0.355 g, 1.0 mmol). The solution was refluxed for 1 h, and an IR spectrum indicated completion of the reaction. After removal of the solvent in vacuo, the residue was redissolved with $CH_2Cl_2$ (10 ml). *n*-Hexane (25 ml) was added to the solution and a yellow-orange solids **2** were formed which were isolated by filtration (G4), washed with *n*-hexane (2 × 10 ml) and subsequently dried under vacuum yielding a mixture of *endo*-, *exo*-[Mo($\eta^3$-$C_3H_5$)($S_2$COEt)(CO)(dppm)] (*endo*-, *exo*-**5**) (0.59 g, 88%) as a yellow-orange microcrystalline solid. Further purification was accomplished by recrystallization from 1/10 $CH_2Cl_2$/*n*-hexane. Spectroscopic data of **5** are as follows. *endo*, *exo*-**5**: IR (KBr, $\upsilon_{CO}$/cm$^{-1}$): 1801(vs). MS (FAB, NBA, *m/z*): 672 ($M^+$), 644 ($M^+-CO$). $^{31}$P{$^1$H} NMR (202 MHz, $CDCl_3$, 298 K): *endo*-**5**: δ 6.9, 32.8 (d, dppm, $^2J_{P-P}$ = 52.7 Hz), *exo*-**5**: δ 3.4, 27.4 (d, dppm, $^2J_{P-P}$ = 63.1 Hz), $^1$H NMR (500 MHz, $CDCl_3$, 298 K): δ 1.10 (t, 3H, $OCH_2CH_3$, $J_{H-H}$ = 11.7 Hz), 2.24, 2.55 (d, 2H, H*anti*, $J_{H-H}$ = 13.3 Hz), 2.42, 4.00 (m, 2H, H*syn*), 3.99, 4.22 (m, 2H, $PCH_2$), 4.01 (m, 2H, $OCH_2CH_3$), 4.91 (m, 1H, H*centre*). $^{13}$C{$^1$H} NMR (125 MHz, $CDCl_3$, 298 K): δ 13.7 (s, $OCH_2CH_3$), 41.5 (t, $PCH_2$, $J_{P-C}$ = 20.5 Hz), 54.7, 68.9 (s, terminal C of allyl), 66.7 (s, $OCH_2$), 100.6 (s, center C of allyl), 222.5 (s, $CS_2$), 227.1 (s, *CO*). MS (FAB, NBA, *m/z*) 671 ($M^+$), 630 ($M^+-C_3H_5$). Anal. Calc. for $C_{32}H_{32}O_2P_2S_2Mo$: C, 57.31; H, 4.81. Found: C, 57.52; H, 4.61%.

### 4.7. Preparation of endo-, exo-**6**

The synthesis and work-up were similar to those used in the preparation of complex *endo*-, *exo*-**5**. The complex *endo*-, *exo*-[Mo($\eta^3$-$C_3H_5$)($S_2$COEt)(CO)(dppe)] (*endo*-, *exo*-**6**) was isolated in 85% yield as a yellow-orange microcrystalline solid. Spectroscopic data of **6** are as follows. IR (KBr, cm$^{-1}$): $\upsilon$(CO) 1798(vs). $^{31}$P{$^1$H} NMR (202 MHz, $CDCl_3$, 298 K): *endo*-**6**: δ 28.7, 32.6 (d, $^2J_{P-P}$ = 26.0 Hz), *exo*-**6**: δ 29.4, 44.8 (d, $^2J_{P-P}$ = 42.2 Hz). *exo*-**6**: $^1$H NMR (200 MHz, $CDCl_3$, 298 K): δ 0.98 (t, 3H, $OCH_2CH_3$, $J_{H-H}$ = 7.0 Hz), 1.44, 1.47 (d, 2H, H*anti*, $J_{H-H}$ = 7.1 Hz), 2.21 (m, 2H, H*syn*), 3.52, 3.77 (m, 4H, $PCH_2$), 4.02 (m, 1H, H*c*), 4.18 (m, 2H, $OCH_2$), 7.06–7.69 (m, 20H, Ph). $^{13}$C{$^1$H} NMR (50 MHz, $CDCl_3$, 298 K): δ 12.6 (s, $OCH_2CH_3$), 25.7 (m, $PCH_2$), 69.9 (s, $OCH_2$), 59.0, 60.5 (s, CH=$CH_2$), 82.5 (s, $CH_2$=CH), 127.1–137.2 (m, Ph), 224.1 (s, $CS_2$), 228.5 (s, CO). MS (FAB, NBA, *m/z*): 686 ($M^+$), 658 ($M^+-CO$). Anal. Calc. for $C_{33}H_{34}O_2P_2S_2Mo$: C, 57.89; H, 5.01. Found: C, 58.06; H, 5.20%.

### 4.8. Preparation of **7**

Dppe (0.198 g, 0.5 mmol) was dissolved in $CH_2Cl_2$ (5 ml) and the solution was added slowly to a flask containing a solution of **1** (0.355 g, 1.0 mmol) in $CH_2Cl_2$ (10 ml) during a period of 5 min. The solution was stirred for 10 min and the solvent was removed in *vacuo* till about 5 ml. Methanol (15 ml) was added to the flask and the solution was stored at −18 °C for 12 h to give yellow precipitates. The precipitate was collected by filtration (G4) washed with *n*-hexane (2 × 10 ml) and then dried in vacuo yielding 0.69 g (96%) of [Mo($\eta^3$-$C_3H_5$)($S_2$COEt)(CO)$_2$]$_2$(μ-dppe)] (**7**). Spectroscopic data of **7** are as follows. IR (KBr, cm$^{-1}$): $\upsilon$(CO) 1942(vs), 1850(vs). $^{31}$P{$^1$H} NMR (202 MHz, $CDCl_3$, 298 K): **7**: δ 29.4 (s, dppe). $^1$H NMR (500 MHz, $CDCl_3$, 298 K): δ 1.40 (t, 3H, $OCH_2CH_3$, $J_{H-H}$ = 7.1 Hz), 4.62 (m, 2H, $OCH_2$), 1.57 (m, 2H, H*anti*), 3.75 (m, 2H, H*syn*), 3.65 (dm, 4H, $PCH_2$, $^2J_{P-H}$ = 35.0 Hz), 4.88 (m, 1H, H*centre*), 7.27–7.60 (m, 20H, Ph). $^{13}$C{$^1$H} NMR (125 MHz, $CDCl_3$, 298 K): δ 14.0 (br, $OCH_2CH_3$), 29.6 (t, $PCH_2$, $J_{P-C}$ = 10.4 Hz), 70.0 (br, $OCH_2$), 60.5 (s, CH=$CH_2$), 82.4 (br, $CH_2$=CH), 128.4–137.2 (m, Ph), 214.0 (s, $CS_2$), 224.1 (s, CO). MS (FAB, NBA, *m/z*): 1026 ($M^+$), 998 ($M^+-CO$). Anal. Calc. for $C_{42}H_{44}O_6P_2S_4Mo_2$: C, 49.12; H, 4.32. Found: C, 49.82; H, 4.53%.

### 4.9. Preparation of endo-, exo-**8**

The synthesis and work-up were similar to those used in the preparation of complex **5**. The complex *endo*-, *exo*-[Mo($\eta^3$-$C_3H_5$)($S_2$COEt)(CO)(dppa)] (*endo*-, *exo*-**8**) was isolated in 92% yield as a yellow-orange microcrystalline solid. Spectroscopic data of **8** are as follows. IR (KBr, cm$^{-1}$): $\upsilon$(CO) 1824(vs). $^{31}$P{$^1$H} NMR (202 MHz, $CDCl_3$, 298 K): *exo*-**8**: δ 62.2, 91.4 (d, $^2J_{P-P}$ = 76.9 Hz), *endo*-**8**: δ 63.2, 98.0 (d, $^2J_{P-P}$ = 63.2 Hz). $^1$H NMR (500 MHz, $CDCl_3$, 298 K): δ 1.00, 1.06 (t, 6H, $OCH_2CH_3$), 2.29, 2.37, 2.62, 2.72 (d, br, 4H, H*anti*, $J_{H-H}$ = 11.6 Hz), 3.50, 3.87, 4.05 (br d, 4H, H*syn*, $J_{H-H}$ = 4.8 Hz), 3.69, 3.97 (m, 4H, $OCH_2$), 5.03, 5.11 (m, 2H, H*centre*), 6.88–7.81 (m, 40H, Ph). $^{13}$C{$^1$H} NMR (125 MHz, $CDCl_3$, 298 K): δ 13.6 (s, $OCH_2CH_3$), 66.9 (s, $OCH_2$), 50.7, 70.5 (s, CH=$CH_2$), 98.0, 102.9 (s, $CH_2$=CH), 126.8–139.3 (m, Ph), 222.9 (s, $CS_2$), 226.6 (s, CO). MS (FAB, NBA, *m/z*): 643 ($M^+-CO$), 602 ($M^+-CO-C_3H_5$). Anal. Calc. for $C_{31}H_{31}NO_2P_2S_2Mo$: C, 55.44; H, 4.65; N, 2.09. Found: C, 55.76; H, 4.30; N, 2.04%.

### 4.10. Single-crystal X-ray diffraction analyses of **1b**, exo-**5**, and endo, exo-**8**

Single crystals of **1b,** *exo*-**5** and *endo, exo*-**8** suitable from X-ray diffraction analyses were grown by recrystallization from 20:1 *n*-hexane/$CH_2Cl_2$. The diffraction data were collected at room temperature on an Enraf-Nonius CAD4 diffractometer equipped with graphite-monochromated Mo Kα ($\lambda$ = 0.71073 Å) radiation. The raw intensity data were converted to structure factor amplitudes and their esd's after correction for scan speed, background, Lorentz, and polarization effects. An empirical absorption correction, based on the azimuthal scan data, was applied to the data. Crystallographic computations were carried out on a Microvax III computer using the NRCC-SDP-VAX structure determination package [18].

A suitable single crystal of **1b** was mounted on the top of a glass fiber with glue. Initial lattice parameters were determined from 24 accurately centered reflections with θ values in the range from 2.10° to 27.50°. Cell constants and other pertinent data were collected and are recorded in Table 1. Reflection data were collected using the $\theta/2\theta$ scan method. Three check reflections were measured every 30 min throughout the data collection and showed no apparent decay. The merging of equivalent and duplicate reflections gave a total of 6230 unique measured data in which 3231 reflections with $I > 2\sigma(I)$ were considered observed. The structure was first solved by using the heavy-atom method (Patterson synthesis), which revealed the positions of metal atoms. The remaining atoms were found in a series of alternating difference Fourier maps and least-squares refinements. The quantity minimized by the least-squares program was $\omega(|F_o| - |F_c|)^2$, where $\omega$ is the

weight of a given operation. The analytical forms of the scattering factor tables for the neutral atoms were used [19]. The non-hydrogen atoms were refined anisotropically. Hydrogen atoms were included in the structure factor calculations in their expected positions on the basis of idealized bonding geometry but were not refined in least squares. All hydrogens were assigned isotropic thermal parameters 1–2 $Å^2$ larger then the equivalent Biso value of the atom to which they were bonded. The final residuals of this refinement were $R = 0.017$ and $Rw = 0.044$. Selected bond distances and angles are listed in Table 2.

The procedures for *exo*-**5** and *endo, exo*-**8** were similar to those for **1b**. The final residuals of this refinement were $R = 0.036$ and $Rw = 0.076$ for *exo*-**5**, and $R = 0.035$ and $Rw = 0.078$ for *endo, exo*-**8**. Selected bond distances and angles are listed in Table 2. Tables of thermal parameters and selected final atomic coordinates are given in the Supplementary material.

## Acknowledgment

We thank the National Science Council of Taiwan, the Republic of China (NSC96-2113-214-001) for support.

## Appendix A. Supplementary material

For **1b**, **5b** and **8** tables of atomic coordinates, crystal and intensity collection data, anisotropic thermal parameters, and bond distances and bond angles. Supplementary data associated with this article can be found, in the online version, at doi:10.1016/j.jorganchem.2008.07.025.

## References

[1] (a) A.J. Graham, R.H. Fenn, J. Organomet. Chem. 17 (1969) 405;
(b) A.J. Graham, R.H.J. Fenn, J. Organomet. Chem. 25 (1970) 173;
(c) F.A. Cotton, B.A. Frenz, A.G. Stanislowski, Inorg. Chim. Acta 7 (1973) 503;
(d) F. Dewans, J. Dewailly, J. Meuniert-Piret, P. Piret, J, Organomet. Chem. 76 (1974) 53.
[2] (a) R.H. Fenn, A.J. Graham, J. Organomet. Chem. 37 (1972) 137;
(b) A.J. Graham, D. Akrigg, B. Sheldrick, Cryst. Struct. Commun. 24 (1976) 173;
(c) F.A. Cotton, C.A. Murillo, B.R. Stults, Inorg. Chim. Acta 7 (1977) 503;
(d) C.A. Cosky, P. Ganis, G. Avatabile, Acta. Crystallogr., Sect. B B27 (1971) 1859;
(e) J.W. Faller, D.F. Chodosh, D. Katahira, J. Organomet. Chem. 187 (1980) 227;
(f) F.A. Cotton, M. Jeremic, A. Shaver, Inorg. Chim. Acta 6 (1972) 543;
(g) B.J. Brisdon, A.A. Woolf, J. Chem. Soc., Dalton Trans. (1978) 291;
(h) B.J. Brisdon, A. Day, J. Organomet. Chem. 221 (1981) 279.
[3] M.D. Curtis, O. Eisenstein, Organometallics 3 (1984) 887.
[4] P. Espinet, R. Hernando, G. Iturbe, F. Villafañe, A.G. Orpen, I. Pascual, Eur. J. Inorg. Chem. (2000) 1031.
[5] K.H. Yih, G.H. Lee, Y. Wang, Inorg. Chem. Commun. 3 (2000) 458.
[6] K.H. Yih, G.H. Lee, S.L. Huang, Y. Wang, Organometallics 21 (2002) 5767.
[7] K.B. Shiu, K.H. Yih, S.L. Wang, F.L.J. Liao, Organomet. Chem. 420 (1991) 359.
[8] K.H. Yih, G.H. Lee, Y. Wang, J. Organomet. Chem. 588 (1999) 125.
[9] K.-H. Yih, S.-C. Chen, Y.-C. Lin, M.-C. Cheng, Y. Wang, J. Organomet. Chem. 494 (1995) 149.
[10] G. Barrado, D. Miguel, V. Riera, S. Garcia-Granda, J. Organomet. Chem. 489 (1995) 129.
[11] (a) B.J. Brisdon, G.F. Griffin, J. Chem. Soc., Dalton Trans. (1975) 1999;
(b) B.J. Brisdon, A.A. Woolf, J. Chem. Soc., Dalton Trans. (1978) 291.
[12] (a) S. Trofimenko, Acc. Chem. Res. 4 (1971) 17;
(b) F.A. Cotton, A.G. Stanislowski, J. Am. Chem. Soc. 96 (1974) 5074;
(c) D.J. Bevan, R.J. Mawby, J. Chem. Soc., Dalton Trans. (1980) 1904.
[13] J.W. Faller, D.A. Haitko, R.D. Adams, D.F. Chodosh, J. Am. Chem. Soc. 101 (1979) 865.
[14] (a) S.K. Chowdhury, M. Nandi, V.S. Joshi, A. Sarkar, Organometallics 16 (1997) 1806 and references cited therein;
(b) M. Kollmar, B. Goldfuss, M. Reggelin, F. Rominger, G. Helmchen, Chem. Eur. J. 7 (2001) 4913.
[15] B.J. Brisdon, D.A. Ewards, K.E. Paddick, M.G.B. Drew, J. Chem. Soc., Dalton Trans. (1980) 1317.
[16] (a) A. Gorfti, M. Salmain, G. Jaouen, M. McGlinchey, A. Bennnouna, A. Mousser, Organometallics 15 (1996) 142;
(b) D.R. van Staveren, T. Weyhermuller, N. Metzler-Nolte, Organometallics 19 (2000) 3730.
[17] R.G. Hayter, J. Organomet. Chem. 13 (1968) P1.
[18] E.J. Gabe, F.L. Lee, Y. Lepage, Crystallographic Computing 3, in: G.M. Sheldrick, C. Kruger, R. Goddard (Eds.), Clarendon Press, Oxford, England, 1985, p. 167.
[19] International Tables for X-ray Crystallography, vol. IV, Reidel: Dordrecht, The Netherlands, 1974.